Therapeutic Activity of Magnesium Oxide Nanoparticles Synthesized by Bacillus Subtilis

Shareef Saleh Al-khateeb[1], Nawfal Hussein Aldujaili[2]
[1, 2] Kufa University, faculty of science, Department of biology, Iraq
E-mail: Njjn629@gmail.com

Abstract
The purpose of this research was to study the biological activity of Magnesium oxide against XDR bacteria Pseudomonas aeruginosa and Staphylococcus aureus MARSA that isolated from burns infections. During the months of August 2022 to December 2022, a total of 75 specimens and investigations were collected. Specimens for burns infection were gathered from two hospitals in the province of AL-Najaf (AL-Hakeem Hospital and Central Laboratory in najaf). Swabs from burns infection patients were collected and sent to the lab, where they were streaked on MacConkey agar, a blood agar., Gram-negative bacteria had a high rate of 58 (78%) based on morphological and biochemical tests, with P. aeruginosa having a high percentage of 39 (52 %) and S. aureus having a high percentage of 15 (20 %). K. pneumonia has 9 (12 %), E. coli has 6 (8%), B.cepacia 3 (4%) , A.baumannii 2(2.67%) and other in 1 (1.33%) . while G +ve bacteria recorded 17 (22 %), with S. aureus being the most isolated bacterium in this investigation. The first diagnosis of bacterial isolates was based on characteristics such as Gram stain, morphology, biochemical testing and automated VTEK-2 . Isolated bacteria were tested against E. coli as an indicator strain for Magnesium Oxide Nanoparticle production. The most effective isolate was chosen based on the colors that change and formation of white precipitation and the biological activity of Mgo NPS against XDR bacteria. B. subtitles S3, was the most effective isolate. Because each microbe has a unique metabolic process and enzyme activity, not all bacteria can manufacture NPs . The characterization of biogenic Mgo NPs was achieved, using UV visible spectrophotometry, Field Emission Scanning electron microscope (FESEM), Energy dispersive spectroscopy (EDS), X-ray diffraction (XRD), and Atomic force microscope (AFM).
Keywords: Nanotechnology , Antibacterial activity of Mgo , XDR bacteria , Anti-biofilm activity of Mgo .

1. Introduction

Nano biotechnology is a growing, interdisciplinary field of research interlacing material science, bio nanoscience and technology. The advances made in the field of nano biotechnology to harness the benefit of life sciences, health care and industrial biotechnology are remarkable (1). Nanoparticles exhibit completely new or improved properties with larger particles of the bulk materials and these novel properties are derived due to the variation in specific characteristics such as size and morphology of the particles (2) . Magnesium oxide (MgO) is an interesting basic metal oxide that has many applications. For example, MgO with ultrafine, nanoscale particles and high specific surface area have shown great promise as destructive adsorbent for toxic chemical agents. Nanoscale MgO exhibits unique optical, electronic, magnetic, thermal, mechanical and chemical properties due to its characteristic structures(19,20).
Chemical synthesized prepared nanoparticles of various methods such as, sol-gel process, micelle, precipitation, hydrothermal and pyrolysis etc. In general, chemicals used for the nanoparticles synthesis and stabilization are toxic and led to non-ecofriendly byproducts are very expensive and use of hazardous chemicals mostly which cause danger to the environment and human beings (3). AMR infections kill over 700,000 people per year across the world. By 2050 up to 10 million people a year could die of antimicrobial resistance(21,22). Aim of study Therapeutic effect of biosynthesized Magnesium oxide nanoparticle against pathogen isolated from wound burn.

2. Materials and Methods

Isolation and identification of bacteria from burn infection

Various types of bacteria were isolated (75 isolates) from burns during the period from August 2022 to December 2022 and diagnosed based on morphology, microscopic examination, biochemical test, and VITEK2 compact system.

Selection the efficient isolate that producing Mgo NPs

Different types of bacterial strains 36 (S1-S36) were screened for biosynthesis of Magnesium oxide NPs, Isolate (S3) was selected as efficient isolate based on color change and antibacterial activity against *P.aeruginosa* and *S. aureus* as indicator strain, S3 diagnosed as *Bacillus subtilis* and depending on the morphology, microscopic examination ,VITEK and molecular detection .Magnesium oxide NPs was synthesized by biological methods using *Bacillus subtilis* by applying $Mg(NO_3)_2$ to each bacteria's cell-free supernatant at a concentration of (0.2 M).

Identification bacterium (S3) was used for the biosynthesis of Mgo NPs

This bacterium (S3) was used for the biosynthesis of

doi.org/10.31838/hiv23.03.119 Received: 20.11.22, Revised: 17.12.22, Accepted: 24.01.23

Mgo NPs and Identification based on: (i)morphological examination (ii)The isolate was identified by VITEK2 with BCL/ID card with 64 biochemical tests.

Characterization of Mgo NPs

The characterization of biogenic Mgo NPs was achieved, using UV visible spectrophotometry, Field Emission Scanning electron microscope (FESEM), Energy dispersive spectroscopy (EDS), X-ray diffraction (XRD), and Atomic force microscope (AFM).

Antibacterial Activity of Mgo NPs

The antibacterial activities of Mgo NPs were tested with different concentration against Extensively drug-Resistant (XDR) bacteria: Gram-negative (*P. aeruginosa) and* Gram-positive *S. aureus MARSA* that isolated from burn infection , bacteria using diffusion method . With 100µl of bacterial suspension, the agar plate was incubated. using a sterile cork Porer, Pores (7 mm diameter) were created and filled with Mgo NPs (100ul) . After that, First , Petri dish were kept at 4 °C for 2h , then incubated at 37°C for 24 hours antibacterial activities was evaluated and the values were provided an means of triplicate by measuring te growth inhibition zone diameter in millimeters.

Ant- biofilm effect by Mgo nanoparticles

In vitro ant biofilm activity was measured using the 96-well microtiter plate technique. The first well microtiter plate filled with 100 µL BHIB broth medium containing 1% glucose and 100 µL of biogenic Mgo NPs then they were made at several diluted concentrations (512,256,128,64,32,16,8,4 and 2 µg/ml), after that we add in each well microtiter plate 100 µL of the diluted concentration till the last one used as a control to confirm the development of biofilm by bacteria and the inhibition of biofilm formation by Mgo NPs. (4)

Antioxidant activity of Mgo nanoparticles

Antioxidant activity evaluation using an offline (DPPH) assay. The DPPH (1,1-diphenyl-2-picrylhydrazyl) radical cation technique that adapted to assess the ability of one hundred pure chemical compounds to scavenge free radicals. The DPPH reagent was DPPH 200 µl as a control in the first well of microplate.

In a 96-well microplate, 100 µL DPPH reagent was mixed with 100 µL of sample (Mgo at different concentration 1000,500,250 and 125 µg/ml) and incubated in dark at room temperature for 30 min to measure scavenging activity. The absorbance was determine at 514 nm using an ELISA reader (TECAN, Grading, Austria) after incubation, using 100 per cent methanol as a blank (5) .The following formula was used to calculate the DPPH scavenging effect:

Radical scavenging (%) = [(*A*)control − (*A*)sample/ (*A*)control] × 100.

3. Results and Discussion

Isolation and identification of Bacteria from burn infections

Seventy-five samples were collected from burns infections. The patients who attending to (AL-Hakeem hospital and the Central Laboratory in najaf). Among the 75 isolates, gram positive cocci, Staphylococcus aureus 15(20%) was the predominant and the most common gram negative bacilli were Pseudomonas aeruginosa 39 (52%) followed by Klebsiella pneumonia 9 (12%), Escherichia coli 6 (8%), B.cepacia 3(4%), A.baumannii 2(2.67%) and others 1 (1.33%) Figure (3-1)

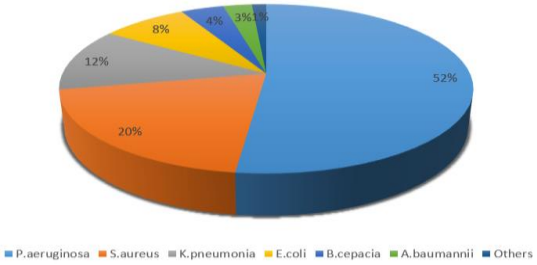

Figure (3-1): Bacterial percentage among clinical samples.
Identification bacterium (S3) was used for the biosynthesis of Mgo NPs.

This bacterium (S3) was used for the biosynthesis of Mgo NPs and Identification as B. subtilis based on: (i)morphological examination, which has a rod shape and is Gram-positive. When cultured on regular nutrient agar, the morphology of this bacteria's spherical colony is rough, fuzzy white, opaque, with jagged edges, In addition, its bacillary shape appeared under a microscope. (ii)The isolate was identified by VITEK2 with BCL/ID card with 64 biochemical tests. The isolate was identified as B. subtilis with probability 91% .

UV-visible Spectroscopy

UV- Visible spectrophotometric is a proven technique for detecting the nanoparticles. After 24 hours of incubation of the reaction mixture, color change was observed which indicated the formation nanoparticles in the reaction mixture. The biosynthesis of nanoparticles can be confirmed by visual observation and measuring the absorbance band using UV-visible spectroscopy. The absorption spectrum of nanoparticles produced in the reaction mixture has a peak at 280nm figure (3- 2) .

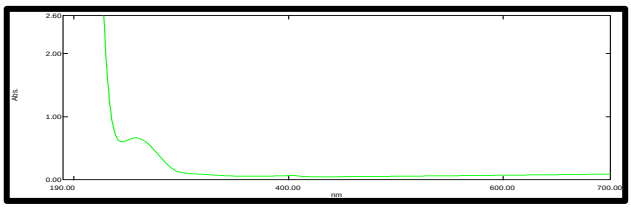

Figure (3-2) UV-visible spectroscopy analysis of Mgo NPs synthesis by B. subtilis

3.2 Field Emission Scanning Electron Microscopy (FESEM) analysis

FESEM used to validate morphology and size of Mgo particles and well distributed and spherical shaped Mgo nanoparticles generated by B. subtilis with a size of between (41.83 – 91.9 nm) the size average of it 66.55 nm. figure (3-3).

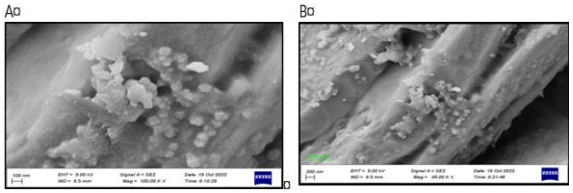

Figure (3-3): FESEM Micrograph of biogenic Mgo nanoparticle synthesized by B. subtilis showed MgoNPs with spherical well scattered with a size average of 66.55 nm. A: at 100 nm B: at 200 nm

Energy dispersive X-Ray spectroscopy (EDS) analysis

The optical absorption peaks of elements were observed using Energy Dispersive Spectroscopy (point and mapping analysis) to quantify the presence of Mgo NPs. The weight percentages of Mgo NPs fabricated by B. subtilis strain were 57.73% oxygen, 18.93 % magnesium, 20.3% phosphor, 0.66 % chloride, 1.03 % sodium, and 1.35 % potassium, as seen in figure (3-4) .

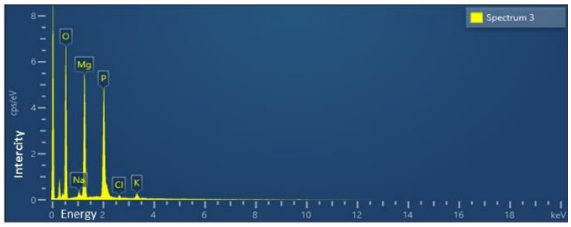

Figure (3-4) EDS analysis of Mgo NPs synthesized by B. subtilis.

Atomic Force Microscope AFM

Atomic force microscopy (AFM) image of Mgo nanoparticle synthesis by B. subtilis , Although the lateral dimensions are influenced by the shape of the probe, the morphology of Mgo NPs was reported. The height measurements be able to provide the elevation of nanoparticles with a high point of precision and accuracy. the average diameter of Mgo NPs biosynthesis from B. subtilis was 13.3nm (3-5) which showed three dimension images, and granularity accumulation distribution charts of Mgo NPs .

Atomic Force Microscopy's extraordinary resolution allows for precise three-dimensional visualization of molecular structures, as well as atomic-scale strategies. The procedure for preparing samples for AFM is straightforward. Because samples can be viewed under near-physiological conditions, AFM can record the critical procedures of molecules, organelles, and other structures in living cells in real time(6)

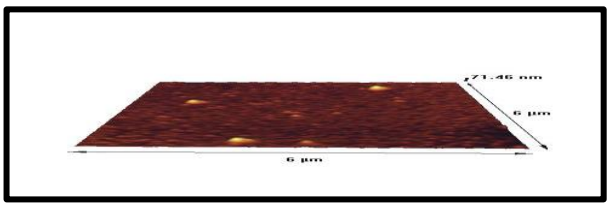

Figure (3-5) AFM analysis of biogenic Mgo synthesis by B. Subtilis

X-Ray diffraction analysis (XRD)

The cubic crystal system of the synthesized MgO was confirmed by the XRD . The 2θ peak positions were well identified with the JCPDS NO: 01-076-1363. Also, the crystalline size was evaluated by the following Debye Scherrer's formula D = 0.94λ/β cosθ. .

The strong peak suggested the inclusion of bioorganic coupons/proteins in the nanoprticles throughout the manufacturing process (Figure 3-6).

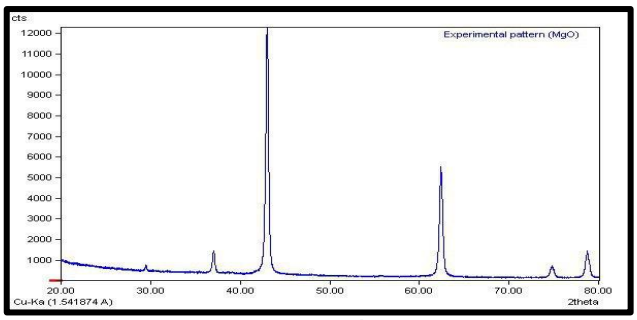

Figure (3-6): XRD analysis of Mgo nanoparticles synthesis by B. subtilis showing the structure and size.

Antibacterial effects of Mgo nanoparticles and antibiotics

The antibacterial activity of biogenic Mgo NPs generated by B. Subtilis against certain Extensive drug resistance (XDR) bacterial pathogens has been tested. The bactericidal activity of biogenic Mgo NPs was determined using the agar well diffusion technique (7).

All of microorganisms studied were inhibited by Mgo NPs at different doses (200, 100 and 50 µg /ml). In Gram negative, largest inhibition zone of Mgo NPs was (20 mm) in P. aeruginosa1 by a concentration of (200 µg /ml), whereas the lowest inhibition zone in Gram positive bacteria was (15 mm) in S. aureus2 at the same concentration. As the quantities of Mgo NPs were raised, the inhibitory impact became stronger. As seen in (Figure 3-7), and table (3-1). It was comparable to earlier studies that found that high concentrations of Mgo NPs inhibited bacterial growth. (8) . The findings revealed that nanoparticles can limit bacterial growth in both Gram- positive and Gram-negative bacteria. Gram- negative bacteria were more sensitive to biogenic Mgo NPs than Gram- positive bacteria.

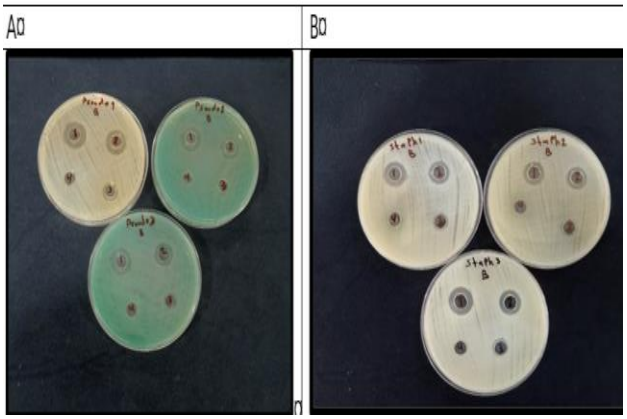

Figure (3-7) Antibacterial activity of Mgo NPs synthesis by B. Subtilis against

A: Three strain from P. aeruginosa. B: Three strain from S. aureus.

Table (3-1) – Inhibition zone of Mgo NPs synthesis by B. Subtilis against three strain from P. aeruginosa. and three strain from S. aureus			
Tested bacteria	inhibition zone (mm)		
	50 µg/ml	100 µg/ml	200 µg/ml
S. aureus 1	10	15	16
S. aureus 2	9	14	15
S. aureus 3	10	16	18
P. aeruginosa 1	12	17	20
P. aeruginosa 2	0	16	17
P. aeruginosa 3	10	15	17

Antibacterial action against many bacteria, including Gram-positive, Gram-negative, aerobic, and anaerobic organism, has been demonstrated. Because these proteins have no harmful impact on humans, they are excellent antibiotic substitutes (9). Current study might suggest that using probiotics that can be a solution to many problems of pathogen antibiotics resistances and can be associated with other options. Which claimed that probiotics are a double-edged sword having both good effects and related hazards, even though probiotics are now considered safe (10). The scientific community has made it their aim to create a successful alternative to replace current antibiotics that have become resistant regions, as well as an effective new entry drug complement to antibiotics, because of the mounting problem of Extensive drug resistance (XDR). Nanoparticles are now being welcomed as a possible alternative to antibiotics, with the potential to solve the bacterial XDR problem (11). In Gram-negative bacteria like P. aeruginosa, as well as Gram-positive bacteria like S. aureus, Mgo NPs is reported to also have antibacterial properties (12). Mgo NPs were shown to be efficient antimicrobial medicines against a wide range of clinically relevant infections. It has been shown that the fundamental mechanism of its antibacterial action is attacking an outer membrane protein called lipopolysaccharide (LPS), which damages cell membranes and causes bacteria to die at neutral PH (13).

The effect of Mgo nanoparticles on haemolysis

Hemolysis is a condition in which red blood cells (RBCs) burst and their components are released, resulting in anemia, jaundice, and renal failure. Because all materials entering the blood come into touch with RBCs, it's critical to assess the materials' hemolytic capacity (14). The hemolysis was identified using Triton X-100 as a positive control indicator. A sterilized phosphate buffer saline solution was employed as a negative control that allowed the stock solution to be stored at room temperature. Mgo NPS throughout all the concentrations (1000, 500, 250, and 125 µg/ml) did not caused hemolysis in the entire blood samples examined as seen in table (3-2) This discovery is with agreement of (Rajkumar et al., 2020) (15) , who found hemolysis did not caused by NPs or solvents in NPs or polymer

Table (3-2) Mgo NPs synthesized by *B. subtilis* effect on hemolysis	
Sample	Hemolysis %
Triton X-100 (positive control)	100
PBS(negative control)	0
Blood with MgoNPs 1000 µg/ml	0
Blood with MgoNPs 500 µg/ml	0
Blood with MgoNPs 250 µg/ml	0
Blood with MgoNPs 125 µg/ml	0
Anti-biofilm effect of Bioactive Mgo NPs.	

Biofilm seems to be the most essential property of bacteria that improves bacterium adhesion to medical equipment and prosthesis surfaces. The antibiofilm efficacy of Mgo NPs generated by B. subtilis was investigated using micro titter plate technique with varied doses of Mgo NPs (512 µg /ml, 256µg/ml, 128 µg /ml, 64 µg /ml, 32 µg /ml, 16 µg /ml, 8 µg /ml, 4 µg /ml) versus three bacteria strains (S. aureus (MARSA) and P. aeruginosa) such as Gram-positive and Gram-negative bacteria.

The antibiofilm effectiveness results differ depending on the harmful bacteria. With the rise in concentration level of Mgo nanoparticles synthesized by B. subtilis and bioactive Mgo showed significant antibiofilm action, at concentration of (512 µg /ml, 256 µg /ml, 128 µg /ml, 64 µg /ml, 32 µg /ml, 16 µg /ml and 8 µg /ml,). The absorption will rise from (100 % to 25%) for S. aureus 1, (99 to 13 %) for S. aureus2 , (99 to 19 %) for S. aureus 3, (99 to 17 %) for P. aeruginosa 1, (99 to 13 %) for P. aeruginosa 2, (100 to 19 %) P. aeruginosa 3 as seen in figure (3-8).

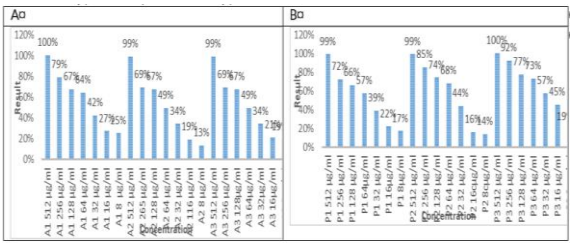

Figure (3-8):Anti-biofilm effect of Mgo NPs synthesised by B. subtilis against pathogenic bacteria A: S. aureus B: P. aeruginosa

Antioxidant activity of Mgo nanoparticles

The DPPH which is (1-Diphenyl-2-picrylhydrazyl), The free radical rummaging experiment performed to determine the antioxidant capacity of MgoNPs metabolites produced from B. subtilis in vitro by decreasing DPPH free radicals. After 30 minutes of introducing nanoparticles at concentrations (1000, 500, 250, and 125 µg/ml) to the DPPH solution, the absorbance at 517 nm was determined. The capacity of nanoparticles to scavenge DPPH free radicals was demonstrated by measuring the colour changes (16) .

DPPH reducing the effect of nanoparticles increased with the elevation in the concentration of biogenic Mgo NPs synthesised by B. subtilis. It was 81% in 1000 µg /ml, 78.9% in 500 µg/ ml, 78% in 250 µg /ml, and 77% in 125 µg/ml for Mgo NPs, figure (3-9).

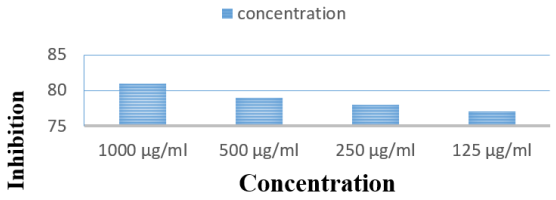

Figure (3-9): Antioxidant effect of Mgo NPs synthesized by B. subtilis in DPPH test.

Traditionally, the antioxidant free radical rummaging capacities of a single 1-diphenyl-2-picrylhydrazyl have been calculated in vitro (DPPH). DPPH appears to be a more stable and well-known free radical, as it is reliant on reducing donor hydrogen or electron absorption. The color change was used to study the efficacy of antioxidants to reduce DPPH (17).

The DPPH rummaging effect of nanoparticles increased as their concentration fell, showing that as the concentration of Mgo NPs decreased, the proportion of DPPH inhibition rise, and that DPPH was inhibited more due to increasing electron donation.

Antioxidants work by searching free radicals and inhibiting their formation. On oxidative stress, free radicals have a strong bactericidal action. Not only has the membrane been destroyed, but biological macromolecules such as proteins, lipids, DNA enzymes, and RNA that trigger cell death have also been harmed (18).

References

Lee, H. J., Yeo, S. Y., & Jeong, S. H. (2003). Antibacterial effect of nanosized silver colloidal solution on textile fabrics. Journal of Materials Science, 38(10), 2199-2204.

P Singh, R., K Shukla, V., S Yadav, R., K Sharma, P., K Singh, P., & C Pandey, A. (2011). Biological approach of zinc oxide nanoparticles formation and its characterization. Advanced Materials Letters, 2(4), 313-317.

Singhal, G., Bhavesh, R., Kasariya, K., Sharma, A. R., & Singh, R. P. (2011). Biosynthesis of silver nanoparticles using Ocimum sanctum (Tulsi) leaf extract and screening its antimicrobial activity. Journal of Nanoparticle Research, 13(7), 2981-2988.

Shakibaie, M., Hajighasemi, E., Adeli-Sardou, M., Doostmohammadi, M., & Forootanfar, H. (2019). Antimicrobial and anti-biofilm activities of Bi subnitrate and BiNPs produced by Delftia sp. SFG against clinical isolates of Staphylococcus aureus, Pseudomonas aeruginosa, and Proteus mirabilis. IET Nanobiotechnology, 13(4), 377–381.

Lee, K. J., Oh, Y. C., Cho, W. K., & Ma, J. Y. (2015). Antioxidant and anti- inflammatory activity determination of one hundred kinds of pure chemical compounds using offline and online screening HPLC assay. Evidence-Based Complementary and Alternative Medicine, 2015.

Deng, X., Xiong, F., Li, X., Xiang, B., Li, Z., Wu, X., Guo, C., Li, X., Li, Y., & Li, G. (2018). Application of atomic force microscopy in cancer research. Journal of Nanobiotechnology, 16(1), 1–15

Alvi, G. B., Iqbal, M. S., Ghaith, M. M. S., Haseeb, A., Ahmed, B., & Qadir, M. I. (2021). Biogenic selenium nanoparticles (SeNPs) from citrus fruit have anti-bacterial activities. Scientific Reports, 11(1), 1–11.

Huang, T., Holden, J. A., Heath, D. E., O'Brien-Simpson, N. M., & O'Connor, A. J. (2019). Engineering highly effective antimicrobial selenium nanoparticles through control of particle size. Nanoscale, 11(31), 14937–14951.

Lu, J., Wu, J., Zhang, C., Zhang, Y., Lin, Y., & Luo, Y. (2018). Occurrence, distribution, and ecological-health risks of selected antibiotics in coastal waters along the coastline of China. Science of the Total Environment, 644, 1469–1476.

Tazehabadi, M. H., Algburi, A., Popov, I. V, Ermakov, A. M., Chistyakov, V. A., Prazdnova, E. V, Weeks, R., & Chikindas, M. L. (2021). Probiotic bacilli inhibit salmonella biofilm formation without killing planktonic cells. Frontiers in Microbiology, 12, 615328.

Morone, M. V., Dell'Annunziata, F., Giugliano, R., Chianese, A., De Filippis, A., Rinaldi, L., Gambardella, U., Franci, G., Galdiero, M., & Morone, A. (2022). Pulsed laser ablation of magnetic nanoparticles as a novel antibacterial strategy against gram positive bacteria. Applied Surface Science Advances, 7, 100213.

Li, Y., Jeon, J., & Park, J. H. (2020). Hypoxia-responsive nanoparticles for tumor-targeted drug delivery. Cancer Letters, 490, 31–43.

Medina Cruz, D., Mi, G., & Webster, T. J. (2018). Synthesis and characterization of biogenic selenium nanoparticles with antimicrobial properties made by Staphylococcus aureus, methicillin-resistant Staphylococcus aureus (MRSA), Escherichia coli, and Pseudomonas aeruginosa. Journal of Biomedical Materials Research Part A, 106(5), 1400–1412.

Swain, P., Das, R., Das, A., Padhi, S. K., Das, K. C., & Mishra, S. S. (2019). Effects of dietary zinc oxide and selenium nanoparticles on growth performance, immune responses and enzyme activity in rohu, Labeo rohita (Hamilton). Aquaculture Nutrition,

25(2), 486–494.
Baravkar, P. N., Sayyed, A. A., Rahane, C. S., Chate, G. P., Wavhale, R. D., Pratinidhi, S. A., & Banerjee, S. S. (2021). Nanoparticle Properties Modulate Their Effect on the Human Blood Functions. BioNanoScience, 11(3), 816–824.
Podder, S., Chanda, D., Mukhopadhyay, A. K., De, A., Das, B., Samanta, A., Hardy, J. G., & Ghosh, C. K. (2018). c. Inorganic Chemistry, 57(20), 12727–12739.
Dawadi, S., Katuwal, S., Gupta, A., Lamichhane, U., Thapa, R., Jaisi, S., Lamichhane, G., Bhattarai, D. P., & Parajuli, N. (2021). Current research on silver nanoparticles: Synthesis, characterization, and applications. Journal of Nanomaterials, 2021.
Peron, S., Hadi, F., Azarbani, F., & Ananda Murthy, H. C. (2021). Antimicrobial, antioxidant, anti-glycation and toxicity studies on silver nanoparticles synthesized using Rosa damascena flower extract. Green Chemistry Letters and Reviews, 14(3), 519–533.
19-Mohammed, H. Q. (2022). Study if Some Biomarkers in Abortion Women Undergoing Intracytoplasmic Sperm Injection (Icsi) Technique. HIV Nursing, 22(2), 1738-1740.
20-khalfa, H. M., al-msaid, H. L., abood, A. H., naji, M. A., & Hussein, S. K. (2020, December). Cellular genetic expression of purinergic receptors in different organs of male rats injected with cyclophosphoamide. In AIP Conference Proceedings (Vol. 2290, No. 1, p. 020033). AIP Publishing LLC.
Almsaid, H., & Khalfa, H. M. (2020). The effect of Ketogenic diet on vitamin D3 and testosterone hormone in patients with diabetes mellitus type 2. Current Issues in Pharmacy and Medical Sciences, 33(4), 202-205.
Hassan, A. B., AL-Msaid, H. L., noori ghani Al-dujaili, A., & Jaffat, H. S. (2020). Measurement of Lipid Profile in Fasting Persons. Medico-legal Update, 20(1), 209.